

# Signal Characteristics, Motor Cortex Engagement, and Classification Performance of Combined Action Observation, Motor Imagery and SSMVEP (CAMS) BCI

Aravind Ravi<sup>ID</sup>, Paul Wolfe, James Tung<sup>ID</sup>, and Ning Jiang<sup>ID</sup>, *Senior Member, IEEE*

**Abstract**— Motor imagery (MI)-based Brain-Computer Interfaces (BCIs) have shown promise in engaging the motor cortex for recovery. However, individual responses to MI-based BCIs are highly variable and relatively weak. Conversely, combined action observation (AO) and motor imagery (MI) paradigms have demonstrated stronger responses compared to AO or MI alone, along with enhanced cortical excitability. In this study, a novel BCI called Combined AO, MI, and Steady-State Motion Visual Evoked Potential (SSMVEP) (CAMS) was proposed. CAMS was designed based on gait observation and imagination. Twenty-five healthy volunteers participated in the study with CAMS serving as the intervention and SSMVEP checkerboard as the control condition. We hypothesized the CAMS intervention can induce observable increases in the negativity of the movement-related cortical potential (MRCP) associated with ankle dorsiflexion. MRCP components, including Bereitschaftspotential, were measured pre- and post-intervention. Additionally, the signal characteristics of the visual and motor responses were quantified. Finally, a two-class visual BCI classification performance was assessed. A consistent increase in negativity was observed across all MRCP components in signals over the primary motor cortex, compared to the control condition. CAMS visual BCI achieved a median accuracy of 83.8%. These findings demonstrate the ability of CAMS BCI to enhance cortical excitability in relation to movement preparation and execution. The CAMS stimulus not only evokes SSMVEP-like activity and sensorimotor rhythm but also enhances the MRCP. These findings contribute to the understanding of CAMS paradigm in enhancing cortical excitability, consistent and reliable classification performance holding promise for motor rehabilitation outcomes and future BCI design considerations.

Received 31 May 2024; revised 27 October 2024 and 3 February 2025; accepted 18 February 2025. Date of publication 21 February 2025; date of current version 7 March 2025. This work was supported in part by the Ontario Early Researcher Award, Natural Sciences and Engineering Research Council of Canada under Grant RGPIN-2022-03878 and in part by the Ontario Graduate Scholarship. (*Corresponding author: James Tung.*)

This work involved human subjects or animals in its research. Approval of all ethical and experimental procedures and protocols was granted by the Office of Research Ethics of the University of Waterloo under Approval No. ORE # 31850.

Aravind Ravi, Paul Wolfe, and James Tung are with the Department of Systems Design Engineering, University of Waterloo, Waterloo, ON N2L 3G1, Canada (e-mail: aravind.ravi@uwaterloo.ca; jtung@uwaterloo.ca).

Ning Jiang is with the West China Hospital, Sichuan University, Chengdu 610041, China.

Digital Object Identifier 10.1109/TNSRE.2025.3544479

**Index Terms**— Brain computer interface (BCI), electroencephalography (EEG), stroke, neurorehabilitation, action observation (AO) therapy, motor imagery (MI), movement related cortical potentials (MRCPs), neuroplasticity, cortical excitability, electromyography.

## I. INTRODUCTION

AS A LEADING cause of long-term acquired disability in adults in the world [1], stroke often leads to debilitating effects, including impaired motor control, cognitive deficits, speech generation or processing difficulties, and altered emotional states [2]. Impaired motor control commonly manifests as hemiplegia and hemiparesis, which leads to loss of sensorimotor function on one side of the body, contralateral to the damaged hemisphere of the brain. After stroke, approximately 20% of the survivors remain dependent on a wheelchair three months post-stroke and approximately 70% walk with reduced capacity [3].

Gait recovery is a major objective in post-stroke rehabilitation wherein high intensity gait training is provided for patients with impairments [4]. Highly customized exercise programs encourage patient's involvement in the therapy, but the results of the expended effort can be slow and limited leading to sub-optimal recovery.

To overcome such limitations, robotic gait devices have been proposed to enable gait rehabilitation with external electromechanical assistance. While robot-assisted gait rehabilitation demonstrated similar clinical effects to conventional therapy [5] these protocols have been criticized for allowing the patients to be too passive, with reduced effort/intent, indicated by lower metabolic activity and muscle activation. The patient's active involvement, collaboration and motivation are key factors that promote efficient motor learning [6]. Previous studies have shown that active training can enhance cortical excitability compared to passive training [7]. Therefore, there is a need to develop a novel rehabilitation strategy to promote active user engagement by utilizing the movement intent.

In conjunction with robotic gait devices, brain computer interfaces (BCIs) based on electroencephalography (EEG) are an attractive approach for rehabilitation as it enables active participation in therapy [2]. BCIs can be especially useful for people with severe disabilities where the central nervous

system remains largely intact, but are unable to communicate due to damage in the peripheral nervous system and/or musculoskeletal systems. A BCI can obtain the patient's volition explicitly from the neurological signals, and utilize them by bypassing the damaged pathways to provide the user with the ability to communicate or interact effectively with their surroundings. BCIs provide novel possibilities for neurorehabilitation for people with neurological disease such as stroke, amyotrophic lateral sclerosis (ALS) or paralysis [8], [9]. EEG is the most popularly used non-invasive method for recording neural activity from the surface of the scalp. EEG based BCIs, paired with robotic gait devices or real-time feedback, provide a novel strategy for active rehabilitation by decoding the user's intention to move their affected limb. Furthermore, the system can provide relevant feedback to enhance user engagement [10].

Visual BCIs based on P300 responses or steady-state visually evoked potentials (SSVEP) have shown successful applications [11], [12]. Recently, BCIs based on steady-state motion visual evoked potential (SSMVEP) have gained interest as they reduce visual discomfort and perform similarly to SSVEP BCIs [13]. This paradigm does not require lengthy user training and little-to-no algorithm calibration, in contrast with BCIs based on motor imagery (MI), commonly investigated in BCI studies for stroke rehabilitation [14]. However, while visual BCIs offer high decoding accuracy for communication and control applications, they alone are incapable of activating or stimulating the sensorimotor areas critical for facilitating motor recovery.

In the context of stroke rehabilitation, sensorimotor rhythm (SMR) and movement-related cortical potentials (MRCP) have been utilized in BCIs to detect motor intent (e.g., mental activities of MI [15]). When paired with congruent motor feedback delivered by methods such as functional electrical stimulation (FES) [16], electrical stimulation of the peroneal nerve [17], or visual feedback [18] has been shown to induce neural plasticity [17], [19]. Although several clinical studies have used MI-BCI approaches, some limitations exist. An estimated 15-30% of users are unable to elicit a sufficiently clear brain response, which is termed as BCI illiteracy [20] [21]. Further, MI-BCI therapies require the patient to maintain sustained attention to the mental imagery task for extended periods of time, which can induce mental fatigue for patients. MI-BCIs also require long training time and calibration for effective real-time application [2]. Patients with severe cognitive impairments who are incapable of sustaining attention, would become ineligible for such therapies. Finally, MI can be imagined in many different ways, potentially leading to high inter-subject and inter-session variability. Therefore, there is a need for a protocol that provides an intuitive task and elicits strong, consistent sensorimotor responses across subjects.

Action observation (AO) therapy has been demonstrated to have positive rehabilitation outcomes in stroke patients [22], [23]. In this type of intervention, participants are shown videos of limb movements and asked to imagine performing them mentally. The observation of actions has been suggested to activate the same brain regions as those involved in motor imagery and execution [24]. Furthermore, studies have suggested that combined AO + MI likely produces stronger

activations of the sensorimotor areas compared to AO or MI alone [25]. Moreover, providing a visual stimulus during MI will likely enhance user engagement and reduce cognitive demand. Recently, there has been an increased interest in using action observation along with motor imagery as a combined approach for post-stroke therapy [26], [27].

Recently, a novel hybrid BCI was introduced combining the benefits of reduced user training while simultaneously stimulating the sensorimotor area [28]. During combined AO + MI of gait, a significant increase in the event-related desynchronization (ERD) at Cz was observed along with an SSMVEP BCI accuracy of 90% on four classes using canonical correlation analysis (CCA). In the current study, this hybrid modality, will be referred to as CAMS BCI. CAMS stands for combined action observation, motor imagery and SSMVEP BCI. It is designed to leverage multiple visual stimuli presented on a computer screen, catering towards a multi-class BCI. A study in [29] investigated classifying left versus right MI of hand grasping movements with SSVEP intermodulation frequencies in a hybrid BCI paradigm. Previous studies have focused on assessing the efficacy of the visual BCI performance, with emphasis on using occipital EEG electrodes. While this is important for assistive control applications, it is unknown if this BCI can induce changes in the movement-related regions of the cortex when used for an extended period of time, which is critical for application in motor rehabilitation.

The Bereitschaftspotential (BP), an early component of the MRCP, is a negative cortical potential which develops 1.5 s prior to the onset of a self-paced movement [30]. Components of the MRCP such as BP and peak-negativity (PN) can be attributed to movement preparation and movement execution. The BP phase is interpreted as the movement preparation phase, and the neural generators involved include the pre-motor cortex (PMC), (pre-)supplementary motor area (SMA), and cingulate motor areas. A steeper decrease in the negative phase (BP2) occurs approximately 0.5 seconds prior to movement onset involving the primary motor cortex (M1) [30], [31]. The maximum amplitude observed around the movement onset, referred as peak negativity (PN) or motor potential, is primarily produced by the contralateral M1. The components of the MRCP have been used by several studies to indicate the induction of cortical plasticity, skill acquisition and motor training [31], [32].

A novel BCI intervention aimed at inducing acute change in cortical excitability based on the CAMS paradigm was proposed in this current study. It was hypothesized that the proposed CAMS intervention would increase cortical excitability in the movement related areas of the cortex. Specifically, an increase in negativity in the components of the MRCP was expected to be observed after a single experiment session of CAMS. Furthermore, this was compared with the SSMVEP checkerboard as a control condition. Next, the signal characteristics of the visual responses and motor responses during the intervention were quantified using the magnitude spectrum and ERD index, respectively. Finally, the two-class visual BCI classification performance of CAMS was quantified using CCA. The remainder of the paper is organized as follows: Section II presents the CAMS stimulus design, experiment

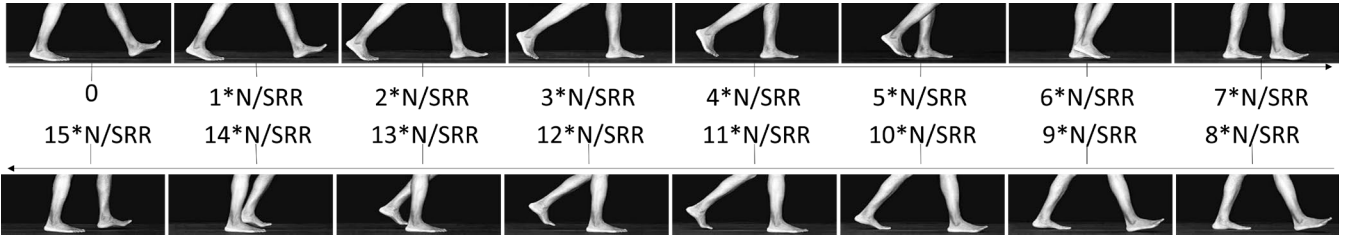


**Fig. 1.** CAMS stimulus generation using sixteen frames corresponding to a single gait cycle.

protocol, EEG data analysis, signal characteristics and classification algorithm. Next, section III presents the results. Finally, section IV discusses the results and concludes the paper.

## II. METHODOLOGY

### A. Data Acquisition

Twenty-five healthy adults (8 F and 17 M, aged 19–45 years) with normal or corrected-to-normal vision volunteered for the experiment. Before starting the experiment, all participants signed a written informed consent. The experiment was approved by the Office of Research Ethics of the University of Waterloo (ORE # 31850).

In this study, EEG and EMG signals were simultaneously acquired from each participant using the g.USBamp and Gammabox (g.tec Guger Technologies, Austria) wet electrode (g.Scarabeo) system with a sampling rate of 1200 Hz. Twelve active EEG electrodes, F3, Fz, F4, FCz, C1, Cz, C2, CPz, POz, O1, O2 and Oz, were used to record from the frontal, central, occipital and occipito-parietal areas according to the International 10-20 system. FPz was used as the ground, and an electrode on the left ear lobe was used as the reference. Additionally, two auxiliary channels recorded the EMG activity sampled at 1200 Hz. Two surface electrodes (720 Series 30\*22mm Ag/AgCl, AMBU, Denmark) were used over the Tibialis Anterior (TA) muscle of the right leg with the ground and reference placed over the medial and lateral malleoli of the ankle, respectively.

### B. Stimulus Design

For this study, two types of repetitive visual stimuli were designed. These two stimuli were the radial checkerboard SSMVEP stimulus and a repetitive gait CAMS stimulus [33]. The SSMVEP stimulus contained a periodic expansion and contraction movement of a checkerboard. Four different repetitive movement frequencies were implemented for this study: 7.5 Hz, 8.57 Hz, 10 Hz and 12 Hz [34]. This stimulus will be referred to as checkerboard/SSMVEP interchangeably.

Next, the CAMS stimulus was designed based on a repetitive gait pattern [33]. Based on a fixed controllable inter-frame interval, a sequence of sixteen frames corresponding to a single cycle were extracted from a video (open source) of gait and presented successively. Figure 1 illustrates the sixteen images used to generate the gait cycle and its detailed implementation can be found in [28]. Each image would last a duration of N frames, before presenting the next frame. The stride frequency

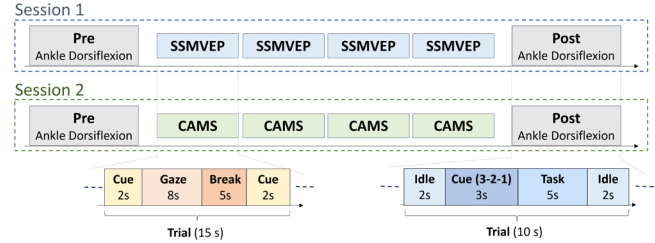


**Fig. 2.** Experiment protocol for the CAMS and SSMVEP stimulus sessions. Sessions were performed with a separation of 24 hours.

(*STF*) was defined as the reciprocal of the time taken to present one full cycle of gait (1). The stimulus frequency (*SF*) was defined as a function of the screen refresh rate (2).

$$STF = \frac{SRR}{(N * NF)} \quad NF = 16; SRR = 60; N = \{5, 6, 7, 8\} \quad (1)$$

$$SF = \frac{SRR}{(N)} \quad SRR = 60; N = \{5, 6, 7, 8\} \quad (2)$$

Four values of the parameter N were implemented: 8, 7, 6 and 5. The SF were: 7.5 Hz, 8.57 Hz, 10 Hz and 12 Hz, similar to the SSMVEP visual frequencies. The estimated *STF* for each case of CAMS were: 0.47 Hz, 0.54 Hz, 0.62 Hz and 0.75 Hz. All stimuli were presented on an LCD screen with a refresh rate of 60 Hz. Overall, the CAMS stimulus was used as the condition under investigation, and the SSMVEP was used as the control condition.

### C. Experimental Protocol

Figure 2 illustrates the overall schema of the experiment protocol. Each participant was required to participate in two sessions, with a minimum 24-hour separation. A single experiment session consisted of three phases of measurements: pre, intervention, and post. The phases of pre- and post-measurements were identical, consisting of thirty-eight ankle dorsiflexions (AD) each, and the intervention-phase consisted of four blocks of the visual stimulus either CAMS or SSMVEP randomly assigned across participants.

1) *Pre/Post Phase*: In both pre- and post-phases of the session, the participant received a visual cue that instructed them to perform one self-paced AD during the trial. A single trial comprised of an idle period of 2 s, cue period of 3 s and task period of 5 s. During the cue period, the participant was provided a countdown from three to one every 1 s as illustrated in Figure 3. They were instructed to perform a single AD anytime during the 5 s task period in a self-paced manner. This protocol was consistent for both sessions across all participants.

\*Code: [https://github.com/uwnrelab/cams\\_bci\\_stimulus\\_generation.git](https://github.com/uwnrelab/cams_bci_stimulus_generation.git)



**Fig. 3.** Pre-/Post-phase cueing screen and CAMS intervention-phase.

**2) Intervention Phase:** During the intervention phase (CAMS or SSMVEP), two visual stimuli were presented on the screen for the two-class BCI, and the participant was directed by a visual cue to gaze at one at a time. The visual stimulus frequencies for these two stimuli were randomly selected from the four frequencies defined earlier. Four paired stimulus frequency combinations out of the six combinations were randomly assigned for each participant. Each trial consisted of a 2 s cue period during which the participant was directed to focus on one of two stimuli displayed on the screen. An 8 s stimulation period followed, where participants were instructed to observe the stimulus for the entire period. Finally, a 5 s break was provided before the start of the next trial.

Each block consisted of 40 stimulus presentations. Each stimulus was presented 20 times during the entire block. Each block lasted 10 minutes. A total of four blocks were performed. In each block, two of four stimulus frequencies were presented in random order, with each frequency presented twice during the entire intervention period. Approximately 3 minutes of resting period was provided between blocks. The stimulus presentation sequence was randomized. The order of the two stimulus conditions was randomized for each participant.

During the CAMS session, participants were instructed, “Observe the gait video as directed by the visual cue and mentally imagine as if you were walking in synchrony with the video; try to synchronize your left and right leg movements with the gait shown in the video.” During the SSMVEP session, participants were instructed to focus on the respective checkerboard stimuli. To reduce movement and ocular artefacts, participants were asked to avoid sudden jerky movements and eye blinks during each trial. The monitor was placed at 55 cm measured between the screen and the eyes of the participant. They were seated in a comfortable chair with both legs rested in a reclined position. Additionally, resting state EEG was collected for 30 s before and after each block. In total, a single session consisted of approximately 40 minutes of intervention-phase, and 15 minutes of pre- and post- measurements, excluding breaks between blocks. The complete experimental protocol was designed and developed in a custom python-based user-interface tool [35]. All data were recorded, stored in comma separated values files and were analyzed offline using Python tools.

#### D. Pre- and Post- Movement Related Cortical Potentials Analysis

EEG and EMG recordings were carefully screened for noisy EEG channels, abrupt changes in peak-to-peak EEG amplitude

and MRCP morphology. Three of twenty-five participants were removed from the analysis due to noisy Cz channel, particularly participants with longer hair. Two more participants were removed from the analysis as the number of good MRCP trials, defined as those that contained a peak-to-peak amplitude of less than 100  $\mu$ V, were less than 30%. Finally, twenty participants were used in the subsequent analysis.

Movement onset of the AD was first detected using a threshold-based approach applied to two EMG channels. First, temporal filtering was applied between 100 Hz and 200 Hz using a 4<sup>th</sup> order Butterworth band-pass filter on both EMG channels. Next, the mean of the signal was subtracted from the filtered signal. To improve the signal-to-noise ratio for movement onset detection, the Teager-Kaiser energy operator (TKEO) [36] was applied on the derived signal. Next, a signal rectification step was applied by taking its absolute value. Finally, through visual inspection, a threshold was empirically identified for each recording, and the first time point that exceeded the threshold was retained as the movement onset time for each AD epoch. The median threshold across sessions and participants for detecting an AD event was 20 mV. Furthermore, the onsets were visually inspected and validated. These movement onsets were subsequently used to select the corresponding AD epochs in the multi-channel EEG signal.

The EEG data from the pre- and post- phases were pre-processed using Independent Component Analysis (ICA) to remove ocular artefacts related to eye movements and blinks [37] using the MNE Python toolbox [38]. After applying ICA, the signals were filtered between 0.01 Hz and 5 Hz using a fourth order zero-phase Butterworth band-pass filter to extract the MRCP activity [39], [40]. The signals were segmented into epochs from 3 s prior to movement onset up to 2 s after. The MRCP was extracted from the channels: C<sub>1</sub>, C<sub>2</sub>, C<sub>z</sub>, FC<sub>z</sub> and CP<sub>z</sub>. Epochs containing an amplitude greater than 105  $\mu$ V (peak-to-peak) were rejected. Baseline correction was applied to all trials in the period between -3 s and -2 s relative to the movement onset. The MRCP was segmented into three regions similar to [31]. From the pre- and post- epochs the following components were extracted from each trial: 1) BP<sub>1</sub> - the mean amplitude of the readiness potential between -1800 milliseconds (ms) and -600 ms, 2) BP<sub>2</sub> - the mean amplitude of the potential between -600 ms and movement onset, and 3) PN - the peak amplitude of the negativity corresponding to the motor potential between -100 ms and 100 ms with respect to the movement onset. Additionally, the slopes of BP<sub>1</sub> and BP<sub>2</sub> were calculated by linear regression to estimate the slope as Slope<sub>1</sub> and Slope<sub>2</sub>, respectively.

#### E. Visual Stimulus Response Characteristics Analysis

Responses in the EEG during the intervention phase for both types of visual stimulus were characterized based on activity elicited in the occipital and motor areas. The magnitude spectrum and signal-to-noise ratio (SNR) were estimated for occipital channels containing steady state visual responses on channels O<sub>1</sub>, O<sub>z</sub> and O<sub>2</sub>. The motor responses were quantified based on the event related desynchronization (ERD) index on channels C<sub>1</sub>, C<sub>z</sub> and C<sub>2</sub>.

First, EEG signals were filtered between 0.5 Hz and 40 Hz using a 4<sup>th</sup> order zero-phase Butterworth band-pass filter. Next, the magnitude spectrum was computed using the Fast Fourier Transform (FFT) applied on the entire 8 s visual stimulation trial at a resolution of 0.09 Hz. The average magnitude spectrum for the four stimulus frequencies (7.5 Hz, 8.57 Hz, 10 Hz and 12 Hz) were each averaged across all participants, trials and channels ( $O_1, O_z, O_2$ ). Next, the SNR was calculated from the magnitude spectrum with respect to the fundamental stimulus frequency for both types of stimuli. For each stimulus frequency  $f$ , SNR was computed as the ratio of the maximum frequency amplitude in the band [ $f - 0.3$  Hz,  $f + 0.3$  Hz] to the mean amplitude of the band [ $f - 2$  Hz,  $f - 0.3$  Hz] and [ $f + 0.3$  Hz,  $f + 2$  Hz], similar to the method used in [13].

To quantify the extent of activity induced in the motor area, the ERD index was computed. The event related spectral perturbation (ERSP) was computed on the EEG trials from channel  $C_1, C_z$  and  $C_2$  based on the multi-taper time frequency approach using the MNE Python toolbox with a time window of 500 ms [41]. The relative changes in spectral power during the trial were obtained by taking the log-ratio between the power in a given frequency band to the power during the baseline period (-1 s to 0 s). Similar to previous studies, the ERD index was calculated and defined in equation (3), where

$$ERD \text{ Index} = 10 \times \log_{10} \frac{P}{R} \quad (3)$$

$P$  is the power during the trial task period and  $R$  is the power in the reference baseline period. This index was used to quantify the degree of EEG band power reduction resulting from a desynchronization of cortical neurons during motor task execution [41], [42]. The frequency bands mu (8 Hz – 12 Hz) and beta (12 Hz to 26 Hz) were quantified in this study.

#### F. CAMS Visual BCI Classifier

Canonical Correlation Analysis (CCA) is the most widely used classifier to detect SSVEP/SSMVEP responses [34], [43], [44], [45]. It is used to estimate the underlying correlation between multi-channel EEG data  $X$  and a set of reference templates  $Y$  of the same length. CCA is used to find the vectors  $w_x$  and  $w_y$  based on the transformations:  $x = X^T w_x$  and  $y = Y^T w_y$  that maximize the correlation between  $x$  and  $y$  by solving (4). Where  $Y_n \in \mathbb{R}^{4 \times N_s}$  are the reference templates (5),  $f_n$

$$\rho(x, y) = \max_{w_x, w_y} \frac{\mathbb{E}[w_x^T X Y^T w_y]}{\sqrt{\mathbb{E}[w_x^T X X^T w_x] \mathbb{E}[w_y^T Y Y^T w_y]}}. \quad (4)$$

$$Y_n = \begin{bmatrix} \sin(2\pi f_n t) \\ \cos(2\pi f_n t) \\ \sin(4\pi f_n t) \\ \cos(4\pi f_n t) \end{bmatrix}, \quad t = \left[ \frac{1}{f_s}, \frac{2}{f_s}, \dots, \frac{N_s}{f_s} \right], \quad (5)$$

where the stimulus frequencies,  $N_s$  defines the number of samples, and  $f_s$  denotes EEG sampling frequency. To classify one of the two CAMS stimulus, the class was assigned as:  $C = \arg\max(\rho_{fi})$ ,  $i = 1, 2$  where  $\rho_{fi}$  were the canonical features extracted for each segment of the EEG.

#### G. Statistical Analysis

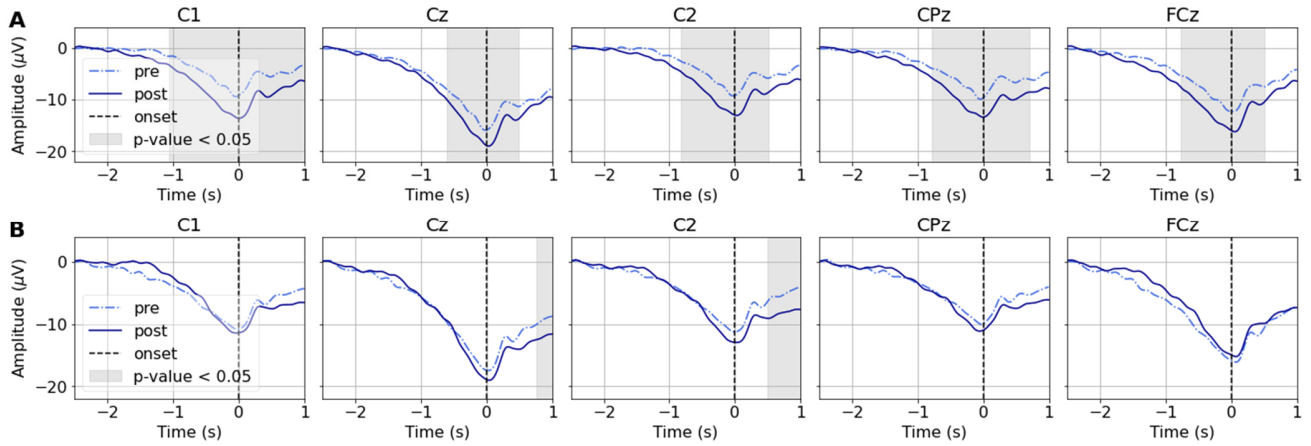
Statistical analysis was performed across participants, trials and stimulus types to compare changes between the pre- and post- measurements. For each stimulus condition, EEG components  $BP_1, BP_2, PN, Slope_1$  and  $Slope_2$  were extracted per trial from the pre- and post- measurements. These were compared individually for each of the five channels:  $C_1, C_z, C_2, FC_z$  and  $CP_z$ , and stimulus types: SSMVEP and CAMS. The comparisons were evaluated with a Mann-Whitney U test with the significance level set to 5%. Furthermore, the temporal differences of the individual MRCP time series between pre- and post- measurements were analyzed using a cluster based permutation test [46], [47] using the built-in MNE function. This was performed on the epoched trials across all participants for each channel and stimulus type. The cluster forming threshold was automatically identified as 3.85 based on  $\alpha$  significance threshold of 0.05 and the number of permutations was set to 1000.

### III. RESULTS

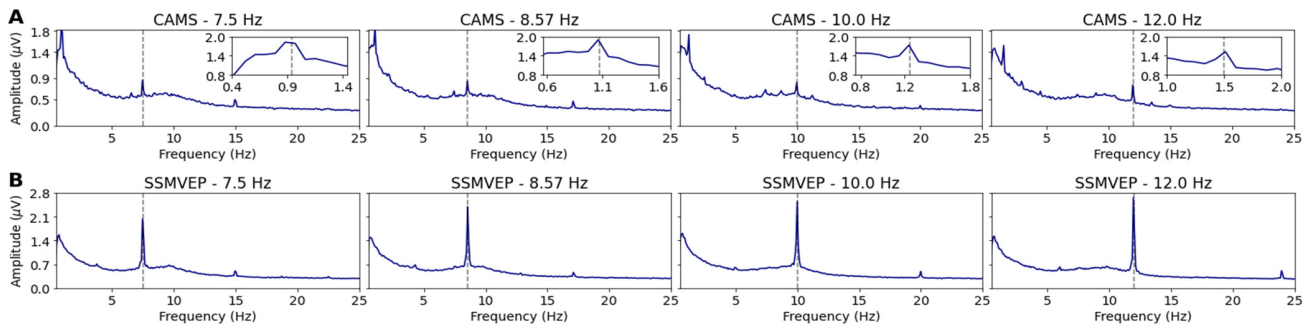
#### A. Pre-/Post- MRCP Measurements CAMS and SSMVEP

Figure 4a and Figure 4b illustrates the grand average MRCP across all participants and trials for all the five channels around  $C_z$  along with the pre- and post- phases for the CAMS and SSMVEP stimuli, respectively. An overall increase in negativity can be observed following the intervention phase across all channels for the CAMS stimulus. Moreover, this increase is consistent across the entire trial duration between -1500 ms to 500 ms with respect to movement onset. An increase in negativity was observed for the components  $BP_1, BP_2$  and  $PN$  for all channels placed over the primary motor cortex ( $C_1, C_z$  and  $C_2$ ) with the greatest differences found for the  $BP_2$  component. In contrast, MRCP components had no significant changes between the pre- and post- measurements for the SSMVEP stimulus condition in most channels; the early components in  $C_1$  and  $FC_z$  showed pre- measurements to be more negative than post- measurements.

Table I summarizes the amplitude differences (post - pre) between the measurements from the pre- and post- phases across the five channels and participants for each MRCP component; C indicates CAMS and S indicates SSMVEP stimulus. An increase in negativity can be readily observed post- intervention across all channels and components for the CAMS stimulus condition. Statistical analyses revealed a significant difference in all five channels  $C_1, C_2, C_z, FC_z$  and  $CP_z$  for the components  $BP_1, BP_2$  and  $PN$  for the CAMS stimulus.  $BP_1$  was (average pre-, post- in  $\mu V \pm$  standard error)  $C_1: (-1.41 \pm 0.54, -3.23 \pm 0.5; p = 0.009)$ ,  $C_z: (-3.74 \pm 0.54, -4.7 \pm 0.5; p = 0.04)$ , and  $C_2: (-1.15 \pm 0.6, -2.66 \pm 0.5; p = 0.04)$ .  $BP_2$  was significantly higher for channels  $C_1: (-6.8 \pm 0.72, -10.95 \pm 0.71; p < 10^{-3})$  and  $C_z: (-11.9 \pm 0.74, -14.8 \pm 0.73; p = p < 10^{-3})$ ,  $C_2: (-6.5 \pm 0.7, -10.2 \pm 0.75; p < 10^{-3})$ . Finally, there was a significant increase in the motor potential  $PN$  in channels  $C_1: (-9.8 \pm 0.8, -14.2 \pm 0.8; p < 10^{-3})$ ,  $C_z: (-16.6 \pm 0.8, -19.6 \pm 0.8; p < 10^{-3})$ , and  $C_2: (-9.9 \pm 0.8, -13.6 \pm 0.8; p = p < 10^{-3})$ . No significant



**Fig. 4.** MRCP averages across participants for the channels C1, Cz, C2, CPz and FCz for 'pre' (light blue) and 'post' (dark blue) conditions for CAMS (A) and SSMVEP (B),  $t = 0$  s (movement onset). Significant differences ( $p < 0.05$ ) highlighted in grey.



**Fig. 5.** Averaged magnitude spectrum for CAMS (A) and SSMVEP (B) responses averaged across channels O1, Oz and O2; all participants for stimulus frequencies: 7.5 Hz, 8.57 Hz, 10 Hz and 12 Hz. Insets for CAMS (A) illustrate responses corresponding to the CAMS step frequency.

changes were identified in the Slope<sub>1</sub> and Slope<sub>2</sub> across all channels for CAMS. For the SSMVEP stimulus, no significant increase in negativity was observed in the MRCP components. The results of cluster based permutation test comparing the epoched trials between the pre- and post- conditions for CAMS revealed significant differences across the channels C<sub>1</sub>, C<sub>2</sub>, C<sub>z</sub>, FC<sub>z</sub> and CP<sub>z</sub>, particularly in the regions between -1000 ms and 250 ms relative to movement onset. No significant changes in negativity were observed in the measurements for the SSMVEP control condition. Furthermore, no significant differences were observed when comparing the time series of the pre- conditions between CAMS and SSMVEP for all channels except FC<sub>z</sub>.

### B. Visual and Motor Responses for CAMS and SSMVEP

1) *Visual Response Characteristics:* Figure 5a and Figure 5b illustrates the averaged magnitude spectrum of the visual steady-state responses recorded during the 8 s visual stimulation phase of the CAMS and SSMVEP stimuli, respectively. The average magnitude spectrum for the stimulus frequencies 7.5, 8.57, 10 and 12 Hz were computed across subjects, trials and channels (O1, O2, Oz) for both stimulus types. Figure 5a shows the magnitude responses corresponding to the fundamental frequency across all participants for the CAMS stimulus. The average amplitude of the dominant peaks were ( $\mu$ V):  $0.88 \pm 0.33$  (7.5 Hz),  $1.65 \pm 0.46$  (8.57 Hz),  $1.8 \pm 0.46$  (10 Hz) and  $1.54 \pm 0.61$  (12 Hz).

$0.87 \pm 0.31$  (8.57 Hz),  $0.82 \pm 0.27$  (10 Hz) and  $0.72 \pm 0.40$  (12 Hz). The insets in Figure 5a illustrate the responses observed in the lower frequency range in the proximity of the respective step frequencies for the CAMS stimulus. These responses averaged across participants were ( $\mu$ V):  $1.65 \pm 0.46$  (7.5 Hz),  $1.8 \pm 0.46$  (8.57 Hz),  $1.6 \pm 0.41$  (10 Hz) and  $1.54 \pm 0.61$  (12 Hz). A strong magnitude response was observed for all four stimulus frequencies for SSMVEP stimulus (Figure 5b) with average magnitude responses ( $\mu$ V):  $1.98 \pm 0.86$  (7.5 Hz),  $2.35 \pm 1.04$  (8.57 Hz),  $2.48 \pm 1.3$  (10 Hz) and  $2.63 \pm 1.13$  (12 Hz). Furthermore, the mean SNR for CAMS were (dB):  $4.07 \pm 2.3$  (7.5 Hz),  $4.01 \pm 2.25$  (8.57 Hz),  $4.05 \pm 1.8$  (10 Hz) and  $4.03 \pm 2.7$  (12 Hz). The SNR for SSMVEP stimulus was (dB):  $10.6 \pm 4.45$  (7.5 Hz),  $12.14 \pm 4.83$  (8.57 Hz),  $12.43 \pm 5.04$  (10 Hz) and  $14.95 \pm 3.8$  (12 Hz).

2) *Motor Responses – Event Related Desynchronization:* Figure 6a (top) displays the averaged event-related desynchronization (ERD) map for the CAMS stimulus averaged across the four stimulus frequencies, participants, trials and channels (C<sub>1</sub>, C<sub>z</sub> and C<sub>2</sub>). Figure 6a (bottom) illustrates the averaged temporal dynamics of the ERD index calculated across the 8 second trial during the CAMS intervention. The median ERD index computed throughout the trial for the mu band was -1.5, beta band was -1.8 and combined mu + beta was -1.7. Figure 6b illustrates the ERD maps (top) and

TABLE I

MRCP COMPONENTS AVERAGED AMPLITUDE DIFFERENCES (POST - PRE) ACROSS THE FIVE CHANNELS C<sub>1</sub>, C<sub>z</sub>, C<sub>2</sub>, FC<sub>z</sub> AND CP<sub>z</sub> ACROSS ALL PARTICIPANTS FOR CAMS (C) AND SSMVEP (S) STIMULUS, \* INDICATES SIGNIFICANT DIFFERENCE ( $P < 0.05$ ) BASED ON THE MANN-WHITNEY U TEST

Channel	BP <sub>1</sub> (μV)		BP <sub>2</sub> (μV)		PN (μV)		Slope <sub>1</sub> (μV/s)		Slope <sub>2</sub> (μV/s)	
	C	S	C	S	C	S	C	S	C	S
C <sub>1</sub>	-1.82*	1.5	-4.15*	-0.1	-4.4*	-0.6	-1.85*	0.16	-1.47	-3.9*
C <sub>z</sub>	-0.96*	0.46	-2.9*	-1.0	-3*	-1.5	-1.05*	-0.45	-1.88	-3.5*
C <sub>2</sub>	-1.51*	0.29	-3.7*	-1.1	-3.7*	-1.7	-1.7*	-0.51	-1.29	-3.7*
FC <sub>z</sub>	-1.7*	1.66	-3.64*	1.1	-3.6*	0.8	-1.68*	0.9	-1.05	-3.03*
CP <sub>z</sub>	-1.35*	0.29	-3.6*	-0.9	-3.68*	-1.1	-1.45*	-0.51	-1.42	-2.6*

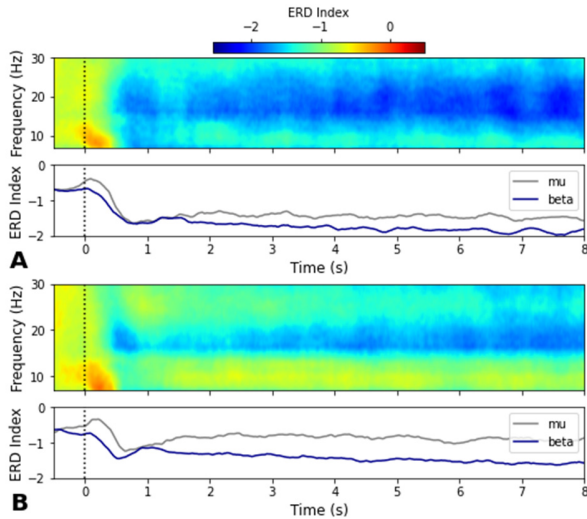


Fig. 6. Average ERDS map and temporal dynamics of the ERD index across all participants, channels (C<sub>1</sub>, C<sub>z</sub>, C<sub>2</sub>) and trials for CAMS (A) and SSMVEP (B) across all stimulus frequencies across the 8 s trial. mu (8 Hz - 12 Hz) and beta (12 Hz - 26 Hz) bands, t = 0 s (onset).

temporal dynamics (bottom) during the stimulation period of the SSMVEP session. The median ERD index calculated for the mu band was  $-0.83$ , beta was  $-1.4$ , and mu + beta was  $-1.25$ . Comparing the ERD indexes between CAMS and SSMVEP, it can be observed that CAMS has a greater ERD index compared to the SSMVEP stimulus in the mu ( $-1.5$  vs  $-0.83$ ), beta ( $-1.8$  vs  $-1.4$ ) and combined ( $-1.7$  vs  $-1.25$ ) bands, respectively. The relative power in the alpha band compared to baseline was higher for SSMVEP than CAMS, likely a result of the volume conduction effects due to visual responses of the checkerboard stimuli appearing on the central electrodes.

### C. CAMS Visual BCI Performance

Figure 7 illustrates the CAMS visual BCI performance for the different two class stimulus frequency combinations for window lengths  $W = 1\text{s}$  to  $W = 8\text{s}$  across all participants. The median accuracies for  $W < 4\text{s}$  were less than 65%, whereas for  $W \geq 4\text{s}$ , the accuracies were greater than 70%. The highest classification accuracies were achieved for  $W = 8\text{s}$  and stimulus combinations (Hz): (8.57, 12) and (7.5,

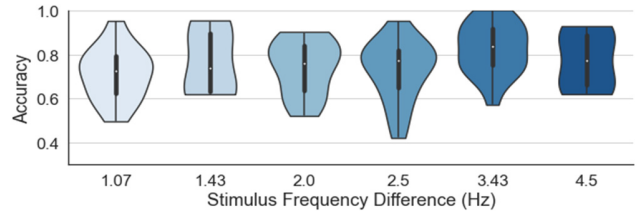


Fig. 7. CAMS visual accuracy vs. stimulus frequency differences for  $W = 8\text{s}$ .

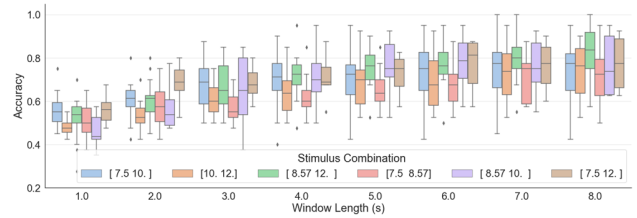


Fig. 8. CAMS visual BCI classification accuracy for each visual stimulus combination, window lengths [1s, 8s] across all participants.

12). Figure 8 presents the classification accuracy considering the frequency differences between the six different stimulus frequency combinations used in this study for  $W = 8\text{s}$ . It is evident that higher classification accuracies were achieved for the stimulus frequencies with greater differences such as 3.43 Hz and 4.5 Hz which correspond to differences between (8.57, 12) and (7.5, 12), respectively. The highest decoding accuracy of 83.8% was achieved for the combination (8.57, 12).

## IV. DISCUSSIONS AND CONCLUSION

### A. CAMS BCI Enhances Cortical Excitability

The results of the pre- and post- measurements clearly indicated that the CAMS BCI intervention enhanced the MRCP components across all channels evident by the increased negativity. This finding can be attributed to an increase in cortical excitability, similar to previous research reporting association between MRCP negativity and cortical excitability [31]. While the effects such as those observed in BP<sub>1</sub>, BP<sub>2</sub> and PN have been studied in tasks involving real movement, including fine motor control tasks [31] and aerobic exercise [32], the integration of AO + MI in this study provides a novel

approach. The observed morphological changes likely reflect contributions from cortical regions such as SMA and M1 [30]. To the authors' best knowledge, this is the first study to examine measures of MRCP in an AO + MI paradigm (CAMS), supporting stronger cortical excitability compared to MI or AO alone.

### B. CAMS Stimulus Activates Visual and Motor Areas

The evidence from this study supports the hypothesis that CAMS elicits stronger activation of the visual and motor areas of the CNS compared to SSMVEP alone. Firstly, a clear fundamental peak and a second harmonic of lower amplitude can be observed in all occipital channels for the CAMS stimulus for all four stimulus frequencies. Next, an interesting and unexpected result was the occurrence of peaks at the lower frequencies between 0.4 Hz and 2 Hz. On further investigation, the peaks illustrated within the insets of Figure 5a were equal to twice the stride frequencies derived from the CAMS stimulus design. This result indicates the occurrence of the step frequency from repetitive gait observation on the occipital EEG electrodes. While this finding is particularly interesting for lower limb tasks, some studies have also shown the manifestation of movement frequencies in the EEG during upper limb tasks [48], [49]. The results of the averaged SSMVEP magnitude spectrum responses indicated a clear peak at the fundamental frequency of the stimulus and a smaller peak at the second harmonic. No other prominent peaks were identified at other frequencies.

The SNR for the CAMS stimulus frequencies were lower than the SSMVEP responses, as expected. Interestingly, the mean SNR was consistent across all frequencies for the CAMS responses. As a result, there is a need to investigate stimulus parameters such as higher frequencies of gait, size, color and contrast influencing the overall SNR of CAMS visual responses. Moreover, this provides opportunities to develop robust and accurate detection algorithms to detect the CAMS response in a visual BCI application.

The motor responses due to the CAMS intervention showed a large ERD, indicating an overall decrease in the power in the mu and beta frequency bands for the entire duration of the trial. This is likely due to cortical activation of M1 and associated areas during congruent action observation and imagination of gait. Although ERD was observed in the SSMVEP intervention, it is lower than the ERD during the CAMS stimulus. Moreover, the ERD during CAMS was sustained throughout the trial for both the mu and beta bands. Overall, these results confirm the simultaneous activation of the motor and occipital cortices evidenced by the ERD and steady state visual responses observed for the CAMS stimulus. Furthermore, the step frequency observed in Figure 5a in the lower end of the magnitude spectrum of CAMS can be beneficial for enhancing the decoding performance of the BCI in future studies.

### C. CAMS Provides High Visual BCI Decoding Accuracy

The CAMS stimulus, characterized by its repetitive gait pattern, notably induces a steady-state response observed in the occipital electrodes, allowing for reliable classification using CCA. While the decoding accuracy was 83.8% (W =

8s), we acknowledge practical considerations that prioritize lower latency and higher speed for effective BCI control applications. These results provide a baseline and motivate future studies to improve the classification performance for lower window lengths. Interestingly, the presentation of two speeds of gait at a reduced frequency difference resulted in lower accuracy. Future inquiry into the effects of frequency differences between stimuli is required for improving the multi-class CAMS BCI paradigm.

### D. Challenges and Limitations

The experiment protocol for the pre- and post- measurements comprised of ~40 trials of AD to measure MRCP, with component calculations performed on a per-trial basis. However, more accurate estimates of MRCP components on an individual subject level can be attained by increasing the number of AD trials. Furthermore, due to the slow frequency nature of the signal, it is susceptible to noise interference. Consequently, up to 30% of trials were rejected for some participants in this study. Hence, future investigations may consider increasing the number of trials to up to 100 for both pre- and post- measurements, while being mindful of the extended experiment duration for participants. The post-measurements were performed within a timeframe of less than four minutes following the conclusion of the last CAMS block. The duration of the observed increase in cortical excitability does not necessarily reflect persistence of these effects over a longer time span.

In this study, recording of MRCPs was performed using only five channels positioned around the Cz electrode. Further investigations to investigate source localization and signal coherence with more channels would provide deeper insight into specific effects. The MRCP was used as a measure to quantify changes in cortical excitability in this study. Although EEG offers a cost-effective and simple setup, it is also highly variable and user dependent. Complementary to the EEG-based approach, future studies replicating the CAMS intervention with transcranial magnetic stimulation (TMS) evoked motor evoked potentials is warranted. Currently, there are few studies that have correlated TMS-elicited metrics with EEG-based measurements, highlighting the necessity for such a comparison study in the future.

An interesting characteristic of the CAMS stimulus is the multi-network nature of the elicited activity. This presents challenges in pinpointing specific neurophysiologic mechanisms at play. Considering the observed changes in the BP and peak negativity components of MRCP, it is likely that cortical excitability changes occurred in the SMA and M1 contralateral to limb movement. The integration of AO + MI in the CAMS stimulus introduced additional modulation of the MRCP by influencing the PN, but also potentially the preparatory components. AO is expected to engage the mirror neuron networks [50], while MI is likely to target networks closely related to those involved in motor planning and execution. Given this close relationship, it is unsurprising that they induce changes in M1, as observed. In order to gain deeper insight into the mechanisms, future research may incorporate paired-pulse TMS to examine neural projections

between cortices. This approach will allow for the investigation of which specific projections may be preferentially targeted by the CAMS stimulus. Furthermore, it will elucidate whether these effects are of purely excitatory nature, and/or imparting their effects via disinhibition.

The CAMS stimulus is a relatively new stimulus design introduced in the literature. Previous studies combining AO with MI have demonstrated increased involvement of the motor cortex when AO is performed from a first-person view compared to a third-person view [51]. However, we implemented a third-person view of gait for the CAMS stimulus. Subsequent investigations can explore the effects of the intervention using a first-person view. Furthermore, the proposed protocol can be extended to upper limb movements [52] and study influence of the CAMS stimulus on cortical regions associated with upper limb movements. Future work can investigate other classification algorithms to improve the visual BCI accuracy for  $W < 4$  s to achieve a faster BCI response for control applications. Additionally, future studies could investigate pure MI or AO control groups to provide a more comprehensive assessment of the CAMS paradigm.

### E. Applications and Conclusion

The results from this study indicate that the proposed CAMS BCI paradigm provides multiple benefits including the ability to enhance cortical excitability within the primary and supplementary motor areas, and providing reliable BCI classification performance. Firstly, the CAMS intervention resulted in an increase in negativity across all MRCP components associated with movement preparation and execution. These findings have implications for motor recovery in individuals with neurological damage affecting the motor cortex [53]. The obtained results substantiate our initial hypothesis that a brief 40-minute intervention employing congruent AO and MI within a BCI can augment motor cortical involvement linked to movement preparation and execution. Future integration of the CAMS system into clinical rehabilitation could involve its use alongside existing assistive devices, such as ankle-foot orthoses, to enhance motor recovery through closed-loop stimulation [15]. Next, the visual decoding accuracy provides a reliable means to develop a BCI that potentially applies for both BCI control and rehabilitation applications. This paradigm holds promise for neuro-rehabilitation applications and helps inform future BCI designs. These findings contribute to understanding the combined AO and MI paradigm in enhancing cortical excitability for motor rehabilitation. Further research is warranted to explore clinical applications and optimize the personalized CAMS BCI paradigm for neurorehabilitation interventions.

### ACKNOWLEDGMENT

The authors thank the participants who took part in this study and the reviewers for their valuable feedback.

### REFERENCES

- [1] W. Johnson, O. Onuma, M. Owolabi, and S. Sachdev, "Stroke: A global response is needed," *Bull. World Health Org.*, vol. 94, no. 9, pp. 634–634, Sep. 2016, doi: [10.2471/BLT.16.181636](https://doi.org/10.2471/BLT.16.181636).
- [2] R. Mane, T. Chouhan, and C. Guan, "BCI for stroke rehabilitation: Motor and beyond," *J. Neural Eng.*, vol. 17, no. 4, Aug. 2020, Art. no. 041001, doi: [10.1088/1741-2552/aba162](https://doi.org/10.1088/1741-2552/aba162).
- [3] O. Lennon et al., "A systematic review establishing the current state-of-the-art, the limitations, and the DESIRED checklist in studies of direct neural interfacing with robotic gait devices in stroke rehabilitation," *Frontiers Neurosci.*, vol. 14, pp. 1–18, Jun. 2020, doi: [10.3389/fnins.2020.00578](https://doi.org/10.3389/fnins.2020.00578).
- [4] J.-M. Belda-Lois et al., "Rehabilitation of gait after stroke: A review towards a top-down approach," *J. NeuroEng. Rehabil.*, vol. 8, no. 1, p. 66, 2011, doi: [10.1186/1743-0003-8-66](https://doi.org/10.1186/1743-0003-8-66).
- [5] J. Hidler et al., "Multicenter randomized clinical trial evaluating the effectiveness of the lokomat in subacute stroke," *Neurorehabil. Neural Repair*, vol. 23, no. 1, pp. 5–13, Jan. 2009, doi: [10.1177/1545968308326632](https://doi.org/10.1177/1545968308326632).
- [6] A. Pennycott, D. Wyss, H. Vallery, V. Klamroth-Marganska, and R. Riener, "Towards more effective robotic gait training for stroke rehabilitation: A review," *J. Neuroengineering Rehabil. (JNER)*, vol. 9, no. 1, p. 65, Jan. 2012, doi: [10.1186/1743-0003-9-65](https://doi.org/10.1186/1743-0003-9-65).
- [7] E. García-Cossío et al., "Decoding sensorimotor rhythms during robotic-assisted treadmill walking for brain computer interface (BCI) applications," *PLoS ONE*, vol. 10, no. 12, Dec. 2015, Art. no. e0137910, doi: [10.1371/journal.pone.0137910](https://doi.org/10.1371/journal.pone.0137910).
- [8] D. Lesenfants et al., "An independent SSVEP-based brain-computer interface in locked-in syndrome," *J. Neural Eng.*, vol. 11, no. 3, Jun. 2014, Art. no. 035002, doi: [10.1088/1741-2550/11/3/035002](https://doi.org/10.1088/1741-2550/11/3/035002).
- [9] X. Zhang, G. Xu, J. Xie, M. Li, W. Pei, and J. Zhang, "An EEG-driven lower limb rehabilitation training system for active and passive co-stimulation," in *Proc. 37th Annu. Int. Conf. IEEE Eng. Med. Biol. Soc. (EMBC)*, Aug. 2015, pp. 4582–4585, doi: [10.1109/EMBC.2015.7319414](https://doi.org/10.1109/EMBC.2015.7319414).
- [10] L. F. Nicolas-Alonso and J. Gomez-Gil, "Brain computer interfaces, a review," *Sensors*, vol. 12, no. 2, pp. 1211–1279, 2012, doi: [10.3390/s120201211](https://doi.org/10.3390/s120201211).
- [11] X. Chen, Y. Wang, M. Nakanishi, X. Gao, T.-P. Jung, and S. Gao, "High-speed spelling with a noninvasive brain-computer interface," *Proc. Nat. Acad. Sci. USA*, vol. 112, no. 44, pp. E6058–E6067, Nov. 2015, doi: [10.1073/pnas.1508080112](https://doi.org/10.1073/pnas.1508080112).
- [12] Y. Wang, X. Gao, B. Hong, C. Jia, and S. Gao, "Brain-computer interfaces based on visual evoked potentials," *IEEE Eng. Med. Biol. Mag.*, vol. 27, no. 5, pp. 64–71, Sep. 2008, doi: [10.1109/memb.2008.92958](https://doi.org/10.1109/memb.2008.92958).
- [13] A. Ravi, J. Lu, S. Pearce, and N. Jiang, "Enhanced system robustness of asynchronous BCI in augmented reality using steady-state motion visual evoked potential," *IEEE Trans. Neural Syst. Rehabil. Eng.*, vol. 30, pp. 85–95, 2022, doi: [10.1109/TNSRE.2022.3140772](https://doi.org/10.1109/TNSRE.2022.3140772).
- [14] A. Ravi, N. H. Beni, J. Manuel, and N. Jiang, "Comparing user-dependent and user-independent training of CNN for SSVEP BCI," *J. Neural Eng.*, vol. 17, no. 2, Apr. 2020, Art. no. 026028, doi: [10.1088/1741-2552/ab6a67](https://doi.org/10.1088/1741-2552/ab6a67).
- [15] R. Xu et al., "A closed-loop brain-computer interface triggering an active Ankle-Foot orthosis for inducing cortical neural plasticity," *IEEE Trans. Biomed. Eng.*, vol. 61, no. 7, pp. 2092–2101, Jul. 2014, doi: [10.1109/TBME.2014.2313867](https://doi.org/10.1109/TBME.2014.2313867).
- [16] C. E. King, P. T. Wang, C. M. McCrimmon, C. C. Chou, A. H. Do, and Z. Nenadic, "The feasibility of a brain-computer interface functional electrical stimulation system for the restoration of overground walking after paraplegia," *J. NeuroEngineering Rehabil.*, vol. 12, no. 1, pp. 1–11, Dec. 2015, doi: [10.1186/s12984-015-0068-7](https://doi.org/10.1186/s12984-015-0068-7).
- [17] N. Mrachacz-Kersting et al., "Efficient neuroplasticity induction in chronic stroke patients by an associative brain-computer interface," *J. Neurophysiology*, vol. 115, no. 3, pp. 1410–1421, Mar. 2016, doi: [10.1152/jn.00918.2015](https://doi.org/10.1152/jn.00918.2015).
- [18] T. Nierhaus, C. Vidaurre, C. Sannelli, K. Mueller, and A. Villringer, "Immediate brain plasticity after one hour of brain-computer interface (BCI)," *J. Physiol.*, vol. 599, no. 9, pp. 2435–2451, May 2021, doi: [10.1113/jphysiol.278118](https://doi.org/10.1113/jphysiol.278118).
- [19] N. Mrachacz-Kersting, S. R. Kristensen, I. K. Niazi, and D. Farina, "Precise temporal association between cortical potentials evoked by motor imagination and afference induces cortical plasticity," *J. Physiol.*, vol. 590, no. 7, pp. 1669–1682, 2012, doi: [10.1113/jphysiol.2011.222851](https://doi.org/10.1113/jphysiol.2011.222851).
- [20] C. Vidaurre and B. Blankertz, "Towards a cure for BCI illiteracy," *Brain Topography*, vol. 23, no. 2, pp. 194–198, Jun. 2010, doi: [10.1007/s10548-009-0121-6](https://doi.org/10.1007/s10548-009-0121-6).

- [21] A. Singh, A. A. Hussain, S. Lal, and H. W. Guesgen, "A comprehensive review on critical issues and possible solutions of motor imagery based electroencephalography brain–computer interface," *Sensors*, vol. 21, no. 6, p. 2173, Mar. 2021, doi: [10.3390/s21062173](https://doi.org/10.3390/s21062173).
- [22] L. R. Borges, A. B. Fernandes, L. P. Melo, R. O. Guerra, and T. F. Campos, "Action observation for upper limb rehabilitation after stroke," *Cochrane Database Systematic Rev.*, vol. 2018, no. 10, Oct. 2018, Art. no. 011887, doi: [10.1002/14651858.cd011887.pub2](https://doi.org/10.1002/14651858.cd011887.pub2).
- [23] G. Buccino, "Action observation treatment: A novel tool in neurorehabilitation," *Phil. Trans. Roy. Soc. B: Biol. Sci.*, vol. 369, no. 1644, Jun. 2014, Art. no. 20130185.
- [24] D. L. Eaves, M. Riach, P. S. Holmes, and D. J. Wright, "Motor imagery during action observation: A brief review of evidence, theory and future research opportunities," *Frontiers Neurosci.*, vol. 10, pp. 1–10, Nov. 2016, doi: [10.3389/fnins.2016.00514](https://doi.org/10.3389/fnins.2016.00514).
- [25] D. J. Wright, J. Williams, and P. S. Holmes, "Combined action observation and imagery facilitates corticospinal excitability," *Frontiers Human Neurosci.*, vol. 8, pp. 1–9, Nov. 2014, doi: [10.3389/fnhum.2014.00951](https://doi.org/10.3389/fnhum.2014.00951).
- [26] J. R. Emerson, J. A. Binks, M. W. Scott, R. P. W. Kenny, and D. L. Eaves, "Combined action observation and motor imagery therapy: A novel method for post-stroke motor rehabilitation," *AMIS Neurosci.*, vol. 5, no. 4, pp. 236–252, 2018, doi: [10.3934/neuroscience.2018.4.236](https://doi.org/10.3934/neuroscience.2018.4.236).
- [27] A. Hioka et al., "Activation of mirror neuron system during gait observation in sub-acute stroke patients and healthy persons," *J. Clin. Neurosci.*, vol. 60, pp. 79–83, Feb. 2019, doi: [10.1016/j.jocn.2018.09.035](https://doi.org/10.1016/j.jocn.2018.09.035).
- [28] X. Zhang, G. Xu, A. Ravi, S. Pearce, and N. Jiang, "Can a highly accurate multi-class SSMVEP BCI induce sensory-motor rhythm in the sensorimotor area?" *J. Neural Eng.*, vol. 18, no. 3, Jun. 2021, Art. no. 035001, doi: [10.1088/1741-2552/ab85b2](https://doi.org/10.1088/1741-2552/ab85b2).
- [29] X. Chi, C. Wan, C. Wang, Y. Zhang, X. Chen, and H. Cui, "A novel hybrid brain–computer interface combining motor imagery and intermodulation steady-state visual evoked potential," *IEEE Trans. Neural Syst. Rehabil. Eng.*, vol. 30, pp. 1525–1535, 2022, doi: [10.1109/TNSRE.2022.3179971](https://doi.org/10.1109/TNSRE.2022.3179971).
- [30] H. Shibasaki and M. Hallett, "What is the bereitschaftspotential?" *Clin. Neurophysiol.*, vol. 117, no. 11, pp. 2341–2356, Nov. 2006, doi: [10.1016/j.clinph.2006.04.025](https://doi.org/10.1016/j.clinph.2006.04.025).
- [31] M. Jochumsen et al., "Quantification of movement-related EEG correlates associated with motor training: A study on movement-related cortical potentials and sensorimotor rhythms," *Frontiers Human Neurosci.*, vol. 11, pp. 1–12, Dec. 2017, doi: [10.3389/fnhum.2017.00604](https://doi.org/10.3389/fnhum.2017.00604).
- [32] J. S. Thacker, L. E. Middleton, W. E. McIlroy, and W. R. Staines, "The influence of an acute bout of aerobic exercise on cortical contributions to motor preparation and execution," *Physiolog. Rep.*, vol. 2, no. 10, Oct. 2014, Art. no. e12178, doi: [10.14814/phy2.12178](https://doi.org/10.14814/phy2.12178).
- [33] A. Ravi, J. Tung, and N. Jiang, "Combined action observation, motor imagery and SSMVEP BCI enhances movement related cortical potential," in *Proc. 11th Int. IEEE/EMBS Conf. Neural Eng. (NER)*, Apr. 2023, pp. 1–4.
- [34] W. Yan et al., "Steady-state motion visual evoked potential (SSMVEP) based on equal luminance colored enhancement," *PLoS ONE*, vol. 12, no. 1, Jan. 2017, Art. no. e0169642, doi: [10.1371/journal.pone.0169642](https://doi.org/10.1371/journal.pone.0169642).
- [35] J. Niu and N. Jiang, "Pseudo-online detection and classification for upper-limb movements," *J. Neural Eng.*, vol. 19, no. 3, Jun. 2022, Art. no. 036042, doi: [10.1088/1741-2552/ac77be](https://doi.org/10.1088/1741-2552/ac77be).
- [36] S. Solnik, P. Rider, K. Steinweg, P. DeVita, and T. Hortobágyi, "Teager–Kaiser energy operator signal conditioning improves EMG onset detection," *Eur. J. Appl. Physiol.*, vol. 110, no. 3, pp. 489–498, Oct. 2010, doi: [10.1007/s00421-010-1521-8](https://doi.org/10.1007/s00421-010-1521-8).
- [37] L. Huang, H. Wang, and Y. Wang, "Removal of ocular artifact from EEG using constrained ICA," *Adv. Eng. Forum*, vols. 2–3, pp. 105–110, Dec. 2011, doi: [10.4028/www.scientific.net/aef.2-3.105](https://doi.org/10.4028/www.scientific.net/aef.2-3.105).
- [38] A. Gramfort, "MEG and EEG data analysis with MNE-Python," *Frontiers Neurosci.*, vol. 7, p. 267, Dec. 2013, doi: [10.3389/fnins.2013.00267](https://doi.org/10.3389/fnins.2013.00267).
- [39] A. Shakeel, M. S. Navid, M. N. Anwar, S. Mazhar, M. Jochumsen, and I. K. Niazi, "A review of techniques for detection of movement intention using movement-related cortical potentials," *Comput. Math. Methods Med.*, vol. 2015, pp. 1–13, Dec. 2015, doi: [10.1155/2015/346217](https://doi.org/10.1155/2015/346217).
- [40] F. Karimi, J. Kofman, N. Mrachacz-Kersting, D. Farina, and N. Jiang, "Detection of movement related cortical potentials from EEG using constrained ICA for brain–computer interface applications," *Frontiers Neurosci.*, vol. 11, pp. 1–10, Jun. 2017, doi: [10.3389/fnins.2017.00356](https://doi.org/10.3389/fnins.2017.00356).
- [41] G. Pfurtscheller and F. H. L. da Silva, "Event-related EEG/MEG synchronization and desynchronization: Basic principles," *Clin. Neurophysiol.*, vol. 110, no. 11, pp. 1842–1857, Nov. 1999, doi: [10.1016/S1388-2457\(99\)00141-8](https://doi.org/10.1016/S1388-2457(99)00141-8).
- [42] K. Aono et al., "Relationship between event-related desynchronization and cortical excitability in healthy subjects and stroke patients," *Tokai J. Experim. Clin. Med.*, vol. 38, no. 4, pp. 123–128, Dec. 2013.
- [43] Z. Lin, C. Zhang, W. Wu, and X. Gao, "Frequency recognition based on canonical correlation analysis for SSVEP-based BCIs," *IEEE Trans. Biomed. Eng.*, vol. 54, no. 6, pp. 1172–1176, Jun. 2007, doi: [10.1109/TBME.2006.889197](https://doi.org/10.1109/TBME.2006.889197).
- [44] M. Nakanishi, Y. Wang, Y.-T. Wang, and T.-P. Jung, "A comparison study of canonical correlation analysis based methods for detecting steady-state visual evoked potentials," *PLoS ONE*, vol. 10, no. 10, Oct. 2015, Art. no. e0140703, doi: [10.1371/journal.pone.0140703](https://doi.org/10.1371/journal.pone.0140703).
- [45] X. Zhang et al., "A convolutional neural network for the detection of asynchronous steady state motion visual evoked potential," *IEEE Trans. Neural Syst. Rehabil. Eng.*, vol. 27, no. 6, pp. 1303–1311, Jun. 2019, doi: [10.1109/TNSRE.2019.2914904](https://doi.org/10.1109/TNSRE.2019.2914904).
- [46] E. Maris and R. Oostenveld, "Nonparametric statistical testing of EEG- and MEG-data," *J. Neurosci. Methods*, vol. 164, no. 1, pp. 177–190, Aug. 2007, doi: [10.1016/j.jneumeth.2007.03.024](https://doi.org/10.1016/j.jneumeth.2007.03.024).
- [47] S. Smith and T. Nichols, "Threshold-free cluster enhancement: Addressing problems of smoothing, threshold dependence and localisation in cluster inference," *NeuroImage*, vol. 44, no. 1, pp. 83–98, Jan. 2009, doi: [10.1016/j.neuroimage.2008.03.061](https://doi.org/10.1016/j.neuroimage.2008.03.061).
- [48] M. Bourguignon, V. Jousmäki, S. S. Dalal, K. Jerbi, and X. De Tiègè, "Coupling between human brain activity and body movements: Insights from non-invasive electromagnetic recordings," *NeuroImage*, vol. 203, Dec. 2019, Art. no. 116177, doi: [10.1016/j.neuroimage.2019.116177](https://doi.org/10.1016/j.neuroimage.2019.116177).
- [49] Y. Wei, X. Wang, R. Luo, X. Mai, S. Li, and J. Meng, "Decoding movement frequencies and limbs based on steady-state movement-related rhythms from noninvasive EEG," *J. Neural Eng.*, vol. 20, no. 6, Dec. 2023, Art. no. 066019, doi: [10.1088/1741-2552/ad01de](https://doi.org/10.1088/1741-2552/ad01de).
- [50] J. J. Q. Zhang, K. N. K. Fong, N. Welage, and K. P. Y. Liu, "The activation of the mirror neuron system during action observation and action execution with mirror visual feedback in stroke: A systematic review," *Neural Plasticity*, vol. 2018, pp. 1–14, Dec. 2018, doi: [10.1155/2018/2321045](https://doi.org/10.1155/2018/2321045).
- [51] S. Ge, H. Liu, P. Lin, J. Gao, C. Xiao, and Z. Li, "Neural basis of action observation and understanding from First- and third-person perspectives: An fMRI study," *Frontiers Behav. Neurosci.*, vol. 12, pp. 1–10, Nov. 2018, doi: [10.3389/fnbeh.2018.00283](https://doi.org/10.3389/fnbeh.2018.00283).
- [52] X. Zhang, W. Hou, X. Wu, S. Feng, and L. Chen, "A novel online action observation-based brains–computer interface that enhances event-related desynchronization," *IEEE Trans. Neural Syst. Rehabil. Eng.*, vol. 29, pp. 2605–2614, 2021, doi: [10.1109/TNSRE.2021.313853](https://doi.org/10.1109/TNSRE.2021.313853).
- [53] T. Mulder, "Motor imagery and action observation: Cognitive tools for rehabilitation," *J. Neural Transmiss.*, vol. 114, no. 10, pp. 1265–1278, Oct. 2007, doi: [10.1007/s00702-007-0763-z](https://doi.org/10.1007/s00702-007-0763-z).